



Observations of Whistler Waves in the Magnetic Reconnection Diffusion Region

S. Y. Huang⁽¹⁾, Z. G. Yuan⁽¹⁾, H. S. Fu⁽²⁾, A. Vaivads⁽³⁾, F. Sahraoui⁽⁴⁾, Y. V. Khotyaintsev⁽³⁾, A. Retino⁽⁴⁾, M. Zhou⁽⁵⁾, D. Graham⁽³⁾, K. Fujimoto⁽⁶⁾, X. H. Deng⁽⁵⁾, B. B. Ni⁽¹⁾, Y. Pang⁽⁵⁾, S. Fu⁽¹⁾, and D. D. Wang⁽¹⁾

(1) School of Electronic Information, Wuhan University, Wuhan, China

(2) Space Science Institute, School of Astronautics, Beihang University, Beijing, China

(3) Swedish Institute of Space Physics, Uppsala, Sweden

(4) Laboratoire de Physique des Plasmas, CNRS-Ecole Polytechnique-UPMC, Palaiseau, France

(5) Institute of Space Science and Technology, Nanchang University, Nanchang, China

(6) Division of Theoretical Astronomy, National Astronomical Observatory of Japan, Mitaka, Tokyo, Japan

Abstract

Whistler waves are believed to play an important role during magnetic reconnection. In this paper, we report the simultaneous occurrence of two types of the whistler waves in the magnetotail reconnection diffusion region. The first type is observed in the pileup region of downstream and propagates away along the field lines to downstream, and is possibly generated by the electron temperature anisotropy at the magnetic equator. The second type is found around the separatrix region and propagates towards the X-line, and is possibly generated by the electron beam-driven whistler instability or Čerenkov emission from electron phase-space holes. Our observations of two different types of whistler waves are well consistent with recent kinetic simulations, and suggest that the observed whistler waves are the consequences of magnetic reconnection. Moreover, we statistically investigate the whistler waves in the magnetotail reconnection region, and construct the global distribution and occurrence rate of the whistler waves based on the two-dimensional reconnection model. It is found that the occurrence rate of the whistler waves is large in the separatrix region ($|B_x/B_0| > 0.4$) and pileup region ($|B_x/B_0| < 0.2$, $|\theta| > 45^\circ$), but very small in the X-line region. The statistical results are well consistent with the case study.

1. Introduction

Magnetic reconnection occurs in a crucial region, called the diffusion region (including ion diffusion region where electrons can be demagnetized and electron diffusion region (EDR) where ions can be demagnetized), where magnetic energy is transferred into plasma kinetic and thermal energy. Strong wave activity and wave-particle interactions in the diffusion region may play an important role in the triggering and development of the reconnection process. Many different types of waves have been observed in or near the reconnection diffusion region, such as electrostatic solitary waves, Langmuir waves, electron cyclotron waves, whistler waves, lower hybrid

waves, kinetic Alfvén waves or Alfvén-whistler waves, and slow magnetosonic waves.

In particular, we focus on whistler waves in this paper. Recent kinetic simulations have pointed out that whistler waves do not control the process of energy dissipation, but are a consequence of the reconnection process itself [Fujimoto and Sydora, 2008]. From the observational view point, Deng and Matsumoto [2001] first reported whistler waves in the vicinity of a reconnection region in the Earth's magnetopause, and treated their observations as evidence of whistler-mediated reconnection. Wei *et al.* [2007] have observed weak whistler waves before the detection of reconnection and strong whistler waves during the reconnection process, leading to the suggestion that the whistler waves may play an important role in triggering the reconnection. Tang *et al.* [2013] have reported whistler waves in the electron diffusion region at the magnetopause, and suggested the whistler waves could heat the electrons. Apart from Tang *et al.* [2013], previous observations have reported whistler waves associated with magnetic reconnection, but have not confirmed the precise locations of the whistler waves and hence the precise roles of these waves during the reconnection process remain unclear.

In this paper, we report the near-simultaneous observations of whistler waves by the Cluster spacecraft in the pileup region and around the separatrix region inside the reconnection diffusion region, and concentrate on the global distribution and the occurrence rate of the whistler waves in the reconnection region using the Cluster data as it can help us to understand their roles and electron dynamics during magnetic reconnection.

2. Observations

The data from several instruments onboard the Cluster spacecraft are used in this study. We revisit the Cluster event on September 19, 2002 studied by Fu *et al.* [2013a]. Two dipolarization fronts (DFs) are detected inside the reconnection region. Figure 1 presents the observations of

the DFs and wave emissions in GSM coordinates measured by Cluster 3 (C3). Two jumps of magnetic field B_z (marked as DF1 and DF2 by vertical dashed lines in Figure 1) were found inside the tailward and earthward flow of the reconnection diffusion region, respectively. These two jumps are identified as DFs.

It can be seen that intense electromagnetic waves (marked by white ellipses in Figure 1) are observed behind both DFs with their frequencies generally below the electron cyclotron frequency f_{ce} , the large polarization degrees (>0.4 in Figure 1f) and positive ellipticities (>0.7 in Figure 1g), and relatively small propagation angles ($<40^\circ$ in Figure 1h). These waves should correspond to the right-hand polarized and quasi-parallel whistler waves. There are no clear whistler waves in the other regions. Therefore, the whistler waves are only observed in the enhancement of magnetic field B_z in the pileup region behind the DFs. Field-aligned Poynting fluxes of whistler waves are mainly positive (Figure 1i), implying that the observed whistler waves propagate parallel to the magnetic field. Then we infer that the whistler waves propagate away from the center of current sheet. For zero guide field reconnection case, the pileup region is generally south-north symmetric, so we can deduce that the source region of the whistler waves should be in the magnetic equator, i.e. the central plane of the current sheet.

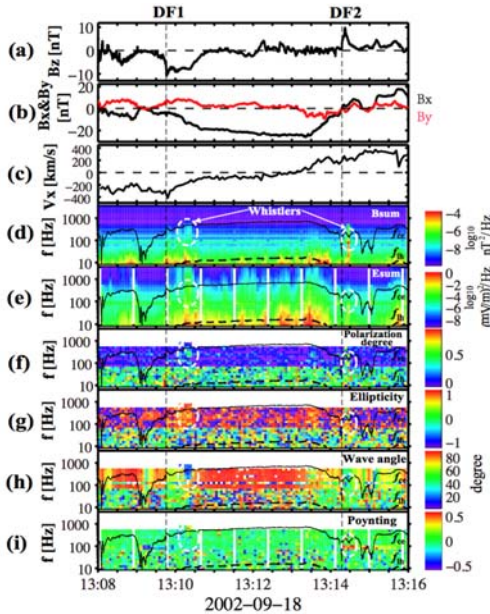


Figure 1. C3 spacecraft measurements of DFs and whistler waves. (a-b) Magnetic field B_z and B_x & B_y components from the FGM instrument. (c) Plasma flow V_x from the CIS experiments; (d-e) Power spectra densities of the magnetic and electric components of the waves. (f) Polarization degrees, (g) ellipticities (red: right hand; blue: left hand), (h) propagation angles, and (i) field-aligned Poynting flux. The parameters in panels (d-i) are from the STAFF instrument. Two vertical dashed lines mark two DFs. The dashed white ellipses emphasize the observations of whistler waves.

Figure 2 shows the observations of the whistler waves detected by Cluster 4 (C4). Two DFs are also observed by C4 (marked as DF1 and DF2 by vertical dashed lines in Figure 2) inside the tailward flow and earthward flow of the reconnection diffusion region, respectively. The jumps in B_z are not very sharp because C4 is far from the current sheet center. Interestingly, electromagnetic whistler waves are also detected, and characterized by their frequencies below electron cyclotron frequency f_{ce} , large polarization degrees (>0.35 in Figure 2f) and right-hand polarized (>0.8 in Figure 2g), and quasi-parallel propagation angles ($<40^\circ$ in Figure 2h). These observations of the whistler waves are highlighted by the white ellipses in Figure 2. Considering the large B_x ($B_x \sim 18$ nT behind DF1 and $B_x \sim 25$ nT behind DF2 in Figure 2b) and small outflow V_x ($|V_x| < 100$ km/s in Figure 2c), we infer that C4 detects the whistler waves far away from the center of the current sheet and around the separatrix region. Field-aligned Poynting fluxes of the whistler waves are positive behind DF1 (northward of the current sheet in the tailward flow) and negative behind DF2 (northward of the current sheet in the earthward flow), indicating that these whistler waves propagate towards the X-line.

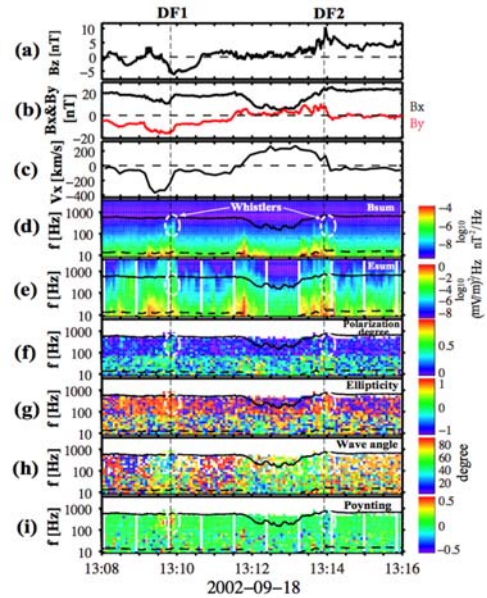


Figure 2. The same format as Figure 1 but for the C4 spacecraft.

We used three bi-Maxwellians to fit the electron distribution behind DF2 when C3 is close to the center of the current sheet. We found see a positive growth rate due to the electron temperature anisotropy with maximum growth $\gamma/\omega_{ce} = 0.003$ occurring at $\omega/\omega_{ce} = 0.252$ (not shown here). From the gyro-resonance condition, the resonant energy is estimated to be 7 keV. The fit to the electron observations agree very well for the electrons near the resonant energies. At these energies the temperature anisotropy is approximately $T_{\perp}/T_{\parallel} = 1.4$, which produces

the observed whistler waves. Thus, the simulated result implies that the whistlers in the pile-up region can be generated by an electron temperature anisotropy. The whistler waves were generated at the separatrix region and propagated towards the X-line by the electron beam instability [Fujimoto, 2014] or the Čerenkov emission from nonlinear coherent electron phase-space holes [Goldman *et al.*, 2014]. We cannot investigate the generation mechanism of these whistlers since C4 detects the whistler waves far from the source region, and the waveforms data are not available in our event. We suggest that the whistlers observed by C4 may be generated by the electron beam-driven whistler instability [Fujimoto 2014], or Čerenkov emissions from electron phase-space holes [Goldman *et al.*, 2014].

To investigate the occurrence rate of whistler waves, we performed statistical study on all magnetotail reconnection events detected by the Cluster. We did normalization on magnetic field by the asymptotic magnetic field B_0 in order to make reasonable comparisons between different reconnection events. For each magnetotail reconnection event, we derived the whistler points based on our aforementioned criteria, and then obtained the ambient magnetic field component B_x and B_z for each whistler wave points. Here the time resolution of one point is 4 s. A two-dimensional distribution of all reconnection points is presented in B_x - B_z plane (Figure 3a) based on the two-dimensional reconnection model [Zhou *et al.*, 2014]. One can see that reconnection points mostly locate around the region of $|B_x/B_0| < 0.8$, $|B_z/B_0| < 0.3$, but cover all over the reconnection region. In our study, thus, we used the below criteria to identify the whistler waves: enhancements of PSDs of electromagnetic field (larger than the instrument noise) in the frequency band: f_{lh} (lower hybrid frequency) $< f < f_{ce}$ (electron cyclotron frequency), polarization degree $P > 0.4$ (quasi-plane wave mode), ellipticity > 0.5 (well right-hand polarization), and propagation angle $\theta < 30^\circ$ (quasi-parallel propagation).

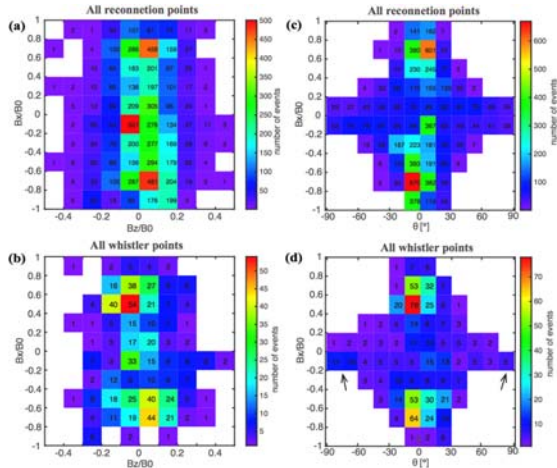


Figure 3. The two-dimensional distributions of (a)(c) all reconnection points and (b)(d) the whistler wave points in

B_x - B_z plane, and B_x - θ plane, respectively. B_x and B_z are normalized by the asymptotic magnetic field B_0 . The number in each bin presents the number of points.

Due to the small magnetic field around the X-line and large $|B_x|$ around the separatrix region, we define the region of $|B_x/B_0| < 0.2$, $|B_z/B_0| < 0.1$ as the vicinity of X-line region (the region is close to the X-line), and the region of $|B_x/B_0| > 0.4$ as the separatrix region. We can see that the whistler waves are mainly detected in the separatrix region and the vicinity of X-line region. We also can present the observations in the B_x - θ plane, where θ is the angle between B_x and B_z , i.e., $\theta = \arctan(B_z/B_x)$. Figure 3c and 3d display all reconnection points and the whistler wave points in B_x - θ plane. Most of reconnection points locate in the region with large $|B_x|$ and small θ . The whistler waves have the similar distribution, i.e., mainly distribute in the region of $|B_x/B_0| > 0.4$ and $|\theta| < 30^\circ$. This region corresponds the separatrix region where $|B_z/B_x| < 1$. There is enhanced B_z component and small amplitude of B_x component in the pileup region. One can see that some whistler waves can be found in the region of $|B_x/B_0| < 0.2$ and $|\theta| > 45^\circ$ (as alleged by the arrows) which can be considered as pileup region.

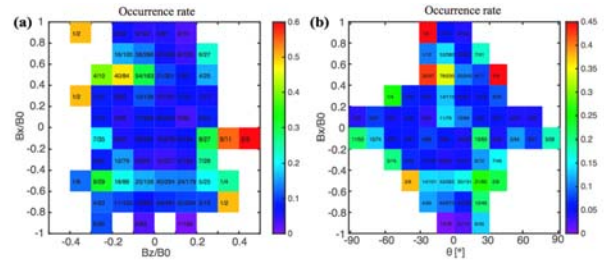


Figure 4. The occurrence rate of the whistle waves in reconnection region in B_x - B_z plane (a), and B_x - θ plane (b).

Dividing the number of sampling points where the whistler waves (N_{whi}) occurred in each bin by the total number of reconnection points (N_{tot}) in the corresponding bin, we obtained the occurrence rate of the whistler waves separately in the reconnection region ($R = N_{whi} / N_{tot}$). The results are shown in the B_x - B_z plane (Figure 4a) and B_x - θ plane (Figure 4b). It can be seen that the maximum occurrence rate of whistler waves in the reconnection region is up to 50%. There are several groups of peak in the occurrence rate in the reconnection region. The first group appears in the region with large B_x ($|B_x/B_0| > 0.4$ in Figure 4a) where the occurrence rate is about 15%-48%. The second group is in the region with small B_x and large B_z ($|B_x/B_0| < 0.2$, $|B_z/B_0| > 0.2$ in Figure 4a) where can be thought as pileup region with the occurrence rate of 20%-66%. Similar features can be also found in Figure 4b. Large occurrence rate is found in the separatrix region of $|B_x/B_0| > 0.4$ and $|\theta| < 30^\circ$, and the pileup region of $|B_x/B_0| < 0.2$ and $|\theta| > 45^\circ$. It is interesting that the occurrence rate is very small, below 8%, in the vicinity of X-line region ($|B_x/B_0| < 0.2$, $|B_z/B_0| < 0.1$ in Figure 4a). This is different with the results in Figure 3b where the number of whistler wave points is considerable. Note that it is

quite difficult to identify the vicinity of X-line region in B_x - θ plane due to large fluctuations in magnetic field in the X-line region. Therefore, we cautiously conclude that the whistler waves were frequently detected in the separatrix region and then pileup region, while much less chance in the vicinity of X-line region.

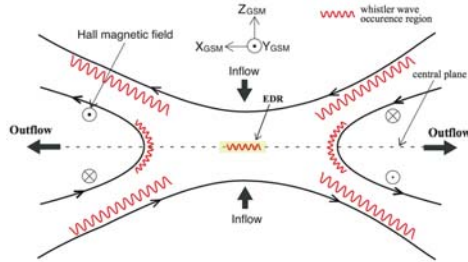


Figure 5. Diagram showing the occurrence region of whistler waves in the reconnection diffusion region. The pink wavy lines display the regions where the whistler waves can be observed. EDR is an abbreviation of electron diffusion region.

We found that the whistler waves have large occurrence rate in the separatrix region and pileup region, while very small occurrence rate in the vicinity of X-line region. Moreover, *Tang et al.* [2013] have shown the whistlers in the electron diffusion region by THEMIS measurements, and we also detected un-negligible distribution of the whistlers in the vicinity of X-line region (in Figure 3b) in this paper. The low occurrence rate in the X-line region or electron diffusion region may be due to that electron diffusion region is rarely small which leads to rarely cross it by the spacecraft, and the limited time resolution of spacecraft data. Here, we conclude that there are three occurrence regions of the whistlers in the reconnection region: separatrix region, pileup region and electron diffusion region (or X-line region). Figure 5 summarizes the occurrence regions of three different types of the whistler waves in the reconnection region.

3. Conclusion

In summary, we observed two types of whistler waves in the reconnection diffusion region. The first type of whistler wave in the pileup region is possibly generated at the magnetic equator by an electron temperature anisotropy, and then propagates away from the source region along the field lines to downstream. The second type of whistler wave around the separatrix is possibly triggered by the electron beam-driven whistler instability or Čerenkov emissions from electron phase-space holes, and propagates towards the X-line. These results are consistent with recent kinetic simulations, and therefore suggest that the observed whistler waves are a result of magnetic reconnection. In addition, we statistically constructed the global distribution and the occurrence rate of the whistler waves in the magnetotail reconnection region. It is found that the occurrence rate is large in the separatrix region ($|B_x/B_0| > 0.4$) and pileup region ($|B_x/B_0| < 0.2$, $|\theta| > 45^\circ$), but low in the vicinity of X-line

region. The statistical results are well consistent with the previous case study and the kinetic simulations.

4. Acknowledgements

This work was supported by the National Natural Science Foundation of China (41374168, 41404132, 41504126, and 41674161), Program for New Century Excellent Talents in University (NCET-13-0446), and China Postdoctoral Science Foundation Funded Project (2015T80830). FS acknowledge financial support from the project THESOW, grant ANR-11-JS56-0008 and from LABEX Plas@Par through a grant managed by the Agence Nationale de la Recherche (ANR), as part of the program “Investissements d’Avenir” under the reference ANR-11-IDEX-0004-02. We thank the Cluster teams and Cluster Science Archive for the high-quality data.

5. References

- Deng, X. H., and H. Matsumoto (2001), Rapid magnetic reconnection in the Earth’s magnetosphere mediated by whistler waves, *Nature*, 410, 557-560.
- Goldman, M. V., et al. (2014), Čerenkov emission of quasiparallel whistlers by fast electron phase-space holes during magnetic reconnection, *Phys. Rev. Lett.*, 112, 145002, doi:10.1103/PhysRevLett.112.145002
- Fujimoto, K., and R. D. Sydora (2008), Whistler waves associated with magnetic reconnection, *Geophys. Res. Lett.*, 35, L19112, doi:10.1029/2008GL035201.
- Fujimoto, K. (2014), Wave activities in separatrix regions of magnetic reconnection, *Geophys. Res. Lett.*, 41, 2721–2728, doi:10.1002/2014GL059893.
- Huang, S. Y., et al. (2016), Two types of whistler waves in the Hall reconnection region, *J. Geophys. Res. Space Physics*, 121, doi:10.1002/2016JA022650. □
- Huang, S. Y., et al. (2017), Occurrence Rate of Whistler Waves in the Magnetotail Reconnection Region, *J. Geophys. Res. Space Physics*, 122, 7188–7196, doi:10.1002/2016JA023670.
- Tang, X., et al. (2013), THEMIS observations of the magnetopause electron diffusion region: Large amplitude waves and heated electrons, *Geophys. Res. Lett.*, 40, 2884–2890, doi:10.1002/grl.50565.
- Wei, X. H., et al., (2007), Cluster observations of waves in the whistler frequency range associated with magnetic reconnection in the Earth’s magnetotail, *J. Geophys. Res.*, 112, A10225, doi:10.1029/2006JA011771.
- Zhou, M., et al., (2014), Characteristic distribution and possible roles of waves around the lower hybrid frequency in the magnetotail reconnection region, *J. Geophys. Res. Space Physics*, 119, 8228–8242, doi:10.1002/2014JA019978.